

# Reaction of $\text{Ni}_2\text{Cp}_2(\mu\text{-CO})_2$ with the Alkylgallium(I) and Alkylindium(I) Compounds $\text{E}_4[\text{C}(\text{SiMe}_3)_3]_4$ ( $\text{E} = \text{Ga}, \text{In}$ ). Insertion of $\text{E-R}$ Groups into the Ni–Ni Bond versus Replacement of CO by the Isolobal $\text{E-R}$ Ligands

Werner Uhl,\* Sandra Melle, Gernot Frenking,\* and Michael Hartmann

Fachbereich Chemie, Philipps-Universität Marburg, Hans-Meerwein-Strasse,  
D-35032 Marburg, Germany

Received June 2, 2000

The monomeric fragment  $\text{In-C}(\text{SiMe}_3)_3$  was inserted into the Ni–Ni bond of  $\text{Ni}_2\text{Cp}_2(\mu\text{-CO})_2$  upon treatment of the carbonyl complex with the tetraindium(I) compound  $\text{In}_4[\text{C}(\text{SiMe}_3)_3]_4$ , **1**, in a molar ratio of 4 to 1. The product (**3**) contains an indium atom coordinated to one alkyl substituent and two  $\text{Ni}(\text{Cp})\text{CO}$  groups in a planar coordination sphere. Reaction of the starting compounds in a molar ratio of 2 to 1 led to the replacement of both CO ligands by two  $\text{InR}$  groups. A compound (**4**) was formed that is isostructural to the carbonyl nickel complex and has a  $\text{Ni}_2$  couple bridged by two  $\text{InR}$  ligands and two terminally coordinated cyclopentadienyl groups. The insertion product was not observed with the gallium derivative  $\text{Ga}_4[\text{C}(\text{SiMe}_3)_3]_4$  (**2**); instead, a nickel gallium complex (**5**) analogous to **4** containing two bridging  $\text{GaR}$  ligands was isolated as the only product regardless of the ratio of the starting compounds. On the basis of quantum chemical calculations, we conclude that there is no evidence for an  $\text{In-In}$  or  $\text{Ga-Ga}$  bond in complexes **4** or **5**, respectively. This, however, supports a butterfly geometry, which is isostructural to the starting carbonyl complex  $\text{Ni}_2\text{Cp}_2(\mu\text{-CO})_2$ .

## Introduction

The alkylelement(I) compounds  $\text{In}_4[\text{C}(\text{SiMe}_3)_3]_4$  (**1**)<sup>1,2</sup> and  $\text{Ga}_4[\text{C}(\text{SiMe}_3)_3]_4$  (**2**)<sup>3</sup> are easily available by the reaction of indium monobromide with the corresponding alkyl lithium derivative or by the reduction of alkyltrichlorogallate(III)(1–) with Rieke magnesium. They possess an almost undistorted tetrahedral cluster of four gallium or indium atoms at their molecular centers. In solution or in the gas phase, the gallium compound **2** dissociates by the formation of the monomeric fragments.<sup>3,4</sup> The indium compound remains a tetramer in solution, but the monomeric fragment was trapped by cycloaddition reactions with benzil derivatives.<sup>5</sup> These monomeric compounds  $\text{E-R}$ <sup>6</sup> are remarkable because they contain coordinatively and electronically highly unsaturated gallium or indium atoms. Their frontier orbitals are similar to those of carbon monoxide, and indeed, we succeeded in replacing bridging CO ligands in transition metal carbonyl complexes by  $\text{InR}$ <sup>7–10</sup> or  $\text{GaR}$ <sup>11</sup> groups. The most exciting complexes obtained

so far are the tetracarbonylnickel analogues  $\text{Ni}[\text{GaC}(\text{SiMe}_3)_3]_4$ <sup>12</sup> and  $\text{Ni}[\text{InC}(\text{SiMe}_3)_3]_4$ <sup>12,13</sup> with terminally coordinated  $\text{E-R}$  ligands for which a significant  $\pi$ -back-bonding of electron density from nickel to empty orbitals at the gallium or indium atoms was verified by quantum chemical calculations.<sup>12</sup> They were obtained by the reaction of bis(cyclooctadiene)nickel with **1** or **2**. The substitution of terminally coordinated CO ligands by  $\text{InR}$  was not observed up to now. Coordination compounds of the transition metals containing elements of group 13 found considerable interest in recent literature; some were employed as precursors for the deposition of alloys from the gas phase.<sup>14</sup> We continued with our investigations in transition metal gallium or indium complexes by treating compounds **1** and **2** with  $\text{Ni}_2\text{-Cp}_2(\mu\text{-CO})_2$  to replace one or both bridging CO ligands. The product of the 2-fold substitution of CO was of particular interest because it may have a butterfly structure similar to the starting carbonyl complex or it may form a tetrahedral  $\text{Ni}_2\text{E}_2$  cluster, which had two electrons more than the tetragallium or tetraindium compounds so that some distortion had to be expected. Quantum chemical calculations using density functional theory are used in order to decide which structural alternative is most suitable for describing these type of complexes.

## Experimental Section

All procedures were carried out under an atmosphere of purified argon in dried solvents (*n*-hexane and cyclopentane over  $\text{LiAlH}_4$ , diisopropyl ether over  $\text{Na/benzophenone}$ ). **1** and **2** were obtained

- (1) Uhl, W.; Graupner, R.; Layh, M.; Schütz, U. *J. Organomet. Chem.* **1995**, *493*, C1.
- (2) Schluter, R. D.; Cowley, A. H.; Atwood, D. A.; Jones, R. A.; Atwood, J. L. *J. Coord. Chem.* **1993**, *30*, 25.
- (3) (a) Uhl, W.; Hiller, W.; Layh, M.; Schwarz, W. *Angew. Chem.* **1992**, *104*, 1378; *Angew. Chem., Int. Ed. Engl.* **1992**, *31*, 1364. (b) Uhl, W.; Jantschak, A. *J. Organomet. Chem.* **1998**, *555*, 263.
- (4) Haaland, A.; Martinsen, K.-G.; Volden, H. V.; Kaim, W.; Waldhör, E.; Uhl, W.; Schütz, U. *Organometallics* **1996**, *15*, 1146.
- (5) Uhl, W.; Keimling, S. U.; Pohl, S.; Saak, W.; Wartchow, R. *Chem. Ber.* **1997**, *130*, 1269.
- (6) A monomeric arylindium(I) compound was recently characterized in the solid state: Haubrich, S. T.; Power, P. P. *J. Am. Chem. Soc.* **1998**, *120*, 2202.
- (7) Uhl, W.; Keimling, S. U.; Hiller, W.; Neumayer, M. *Chem. Ber.* **1995**, *128*, 1137.
- (8) Uhl, W.; Pohlmann, M. *Organometallics* **1997**, *16*, 2478.
- (9) Uhl, W.; Keimling, S. U.; Pohlmann, M.; Pohl, S.; Saak, W.; Hiller, W.; Neumayer, M. *Inorg. Chem.* **1997**, *36*, 5478.

- (10) Uhl, W.; Keimling, S. U.; Hiller, W.; Neumayer, M. *Chem. Ber.* **1996**, *129*, 397.
- (11) Uhl, W.; Benter, M.; Prött, M. *J. Chem. Soc., Dalton Trans.*, in press.
- (12) Uhl, W.; Benter, M.; Melle, S.; Saak, W.; Frenking, G.; Uddin, J. *Organometallics* **1999**, *18*, 3778.
- (13) Uhl, W.; Pohlmann, M.; Wartchow, R. *Angew. Chem.* **1998**, *110*, 1007; *Angew. Chem., Int. Ed. Engl.* **1998**, *37*, 961.
- (14) Review: Fischer, R. A.; Weiss, J. *Angew. Chem.* **1999**, *111*, 3003; *Angew. Chem., Int. Ed.* **1999**, *38*, 2830.

according to literature procedures.<sup>1,3b</sup> Commercially available Ni<sub>2</sub>Cp<sub>2</sub>(μ-CO)<sub>2</sub> (Aldrich) contains nickelocene among others as a very volatile impurity and was sublimed in a vacuum prior to use (100 °C, 10<sup>-3</sup> Torr).

**(Me<sub>3</sub>Si)<sub>3</sub>C–In(NiCpCO)<sub>2</sub> (3).** A solution of 0.513 g (0.371 mmol, excess) of tetraindane(4), **1**, in 35 mL of *n*-hexane was added to a solution of 0.337 g (1.110 mol) of Ni<sub>2</sub>Cp<sub>2</sub>(CO)<sub>2</sub> in 40 mL of *n*-hexane. The solution was heated under reflux for 1 h. The color changed to dark-red, and a black powder precipitated. After filtration, the solvent was distilled off in a vacuum at room temperature. The residue was recrystallized from cyclopentane (20/–50 °C) to yield compound **3** as an amorphous red solid. Yield: 0.437 g (61%, based on the nickel compound). Mp (argon, closed capillary): 128 °C. MS (CI, isobutane): *m/z* 619.9 (100%, M<sup>+</sup> – CO), 497.0 (82%, M<sup>+</sup> – NiCpCO). Molar mass (cryoscopically in benzene): calcd 649.99. Found 635. <sup>1</sup>H NMR (C<sub>6</sub>D<sub>6</sub>, 300 MHz): δ 5.09 (s, Cp), 0.43 (s, SiMe<sub>3</sub>). <sup>13</sup>C NMR (C<sub>6</sub>D<sub>6</sub>, 75.5 MHz): δ 190.9 (s, CO), 91.0 (s, Cp), 43.6 (s, InC), 6.7 (s, SiMe<sub>3</sub>). IR (paraffin, CsBr plates, cm<sup>-1</sup>): 1964 s, 1948 m ν(CO); 1462 vs, 1377 vs paraffin; 1343 m, 1254 s δ(CH<sub>3</sub>); 1169 w, 1109 vw, 1057 w, 1049 w, 1011 w, 988 w ν(CC,Cp); 855 vs, 839 vs, 804 s, 793 vs, 783 s, 721 m ρ(CH<sub>3</sub>(Si)); 675 m, 650 m ν<sub>as</sub>(SiC); 615 vw ν<sub>s</sub>(SiC); 586 m ν(InC); 490 sh, 476 s ν(InC). UV/vis (*n*-hexane, nm, log ε): 220 (4.0), 290 (3.4), 360 (3.1). Anal. Calcd for C<sub>22</sub>H<sub>37</sub>O<sub>2</sub>Si<sub>3</sub>Ni<sub>2</sub>In: Ni, 18.1; In, 17.7. Found: Ni, 18.0; In, 17.4.

**[CpNi{μ–InC(SiMe<sub>3</sub>)<sub>3</sub>}<sub>2</sub>NiCp] (4).** Predried *n*-hexane and diisopropyl ether were further dried over *n*-butyllithium and freshly distilled prior to use. A solution of In<sub>4</sub>[C(SiMe<sub>3</sub>)<sub>3</sub>]<sub>4</sub>, **1** (0.341 g, 0.247 mmol, excess), in 25 mL of *n*-hexane was added to a solution of Ni<sub>2</sub>Cp<sub>2</sub>(CO)<sub>2</sub> (0.100 g, 0.329 mmol) in 25 mL of *n*-hexane. The solution was heated under reflux for 1 h. The color changed from violet of **1** to dark-red. A black solid precipitated, which was filtered off. The filtrate was concentrated in a vacuum at room temperature and cooled to –50 °C to obtain red needles of compound **4**. **4** is very hygroscopic in solution. Yield: 0.203 g (66% based on the carbonylnickel compound). Mp (argon, closed capillary): 125 °C (dec). <sup>1</sup>H NMR (C<sub>6</sub>D<sub>6</sub>, 300 MHz): δ 5.22 (s, Cp), 0.34 (s, SiMe<sub>3</sub>). <sup>13</sup>C NMR (C<sub>6</sub>D<sub>6</sub>, 75.5 MHz): δ 84.2 (Cp), 46.8 (InC), 5.8 (SiMe<sub>3</sub>). IR (paraffin, CsBr plates, cm<sup>-1</sup>): 1287 vw, 1252 s δ(CH<sub>3</sub>); 1113 vw, 1082 vw, 1044 w, 1007 w ν(CC, Cp); 858 vs, 841 vs, 789 m, 781 m, 723 w ρ(CH<sub>3</sub>(Si)); 673 m, 652 w ν<sub>as</sub>(SiC); 615 w ν<sub>s</sub>(SiC); 598 w ν(InC); 519 w, 463 w ν(InC); 359 vw δ(SiC). UV/vis (*n*-hexane, nm, log ε): 225 (4.0), 295 (sh, 3.5), 340 (sh, 3.2), 435 (sh, 2.6), 580 (1.9). Anal. Calcd for C<sub>30</sub>H<sub>64</sub>Si<sub>6</sub>Ni<sub>2</sub>In<sub>2</sub>: Ni, 12.5; In, 24.4. Found: Ni, 12.2; In, 24.3.

**[CpNi{μ–GaC(SiMe<sub>3</sub>)<sub>3</sub>}<sub>2</sub>NiCp] (5).** *n*-Hexane and diisopropyl ether were additionally dried over *n*-butyllithium and freshly distilled prior to use. A solution of 0.078 g (0.257 mmol) of Ni<sub>2</sub>Cp<sub>2</sub>(CO)<sub>2</sub> in 20 mL of *n*-hexane was treated with a solution of 0.155 g (0.129 mmol) of tetragallane(4), **2**, in 20 mL of *n*-hexane and heated under reflux for 2.5 h. The dark-red solution was concentrated in a vacuum at room temperature and cooled to –30 °C to obtain dark-red needles of compound **5**, which is very moisture-sensitive in solution. Yield: 0.133 g (61%). Mp (argon, closed capillary): 137 °C (dec). <sup>1</sup>H NMR (C<sub>6</sub>D<sub>6</sub>, 300 MHz): δ 5.25 (s, Cp), 0.38 (s, SiMe<sub>3</sub>). <sup>13</sup>C NMR (C<sub>6</sub>D<sub>6</sub>, 75.5 MHz): δ 87.2 (Cp), 43.4 (GaC), 5.8 (SiMe<sub>3</sub>). IR (paraffin, CsBr plates, cm<sup>-1</sup>): 1339 vw, 1290 vw, 1260 s, 1250 s δ(CH<sub>3</sub>); 1169 vw, 1159 vw, 1119 vw, 1111 vw, 1087 vw, 1047 w, 1005 m ν(CC,Cp); 855 vs, 793 vs, 787 vs, 772 s ρ(CH<sub>3</sub>(Si)); 675 m, 654 s ν<sub>as</sub>(SiC); 625 m ν(GaC); 615 sh ν<sub>s</sub>(SiC); 590 vw, 521 vw, 463 w ν(GaC); 376 vw, 330 w δ(SiC). UV/vis (*n*-hexane, nm, log ε): 210 (3.7), 245 (3.6), 280 (sh, 3.4), 470 (2.5). Anal. Calcd for C<sub>30</sub>H<sub>64</sub>Si<sub>6</sub>Ni<sub>2</sub>Ga<sub>2</sub>: Ni, 13.8; Ga, 16.4. Found: Ni, 14.1; Ga, 16.5.

**Crystal Structure Determinations.** Single crystals were obtained by recrystallization from cyclopentane (**3**, 20/–30 °C) and diisopropyl ether (very slow cooling to –30 °C (**4**) or 0 °C (**5**)). The X-ray data collections were performed on four-circle diffractometer AED 2 (**3**) and STOE IPDS systems (**4** and **5**) with graphite-monochromated Mo Kα radiation. The crystals (**3**, 1.1 mm × 0.6 mm × 0.2 mm; **4**, 0.8 mm × 0.7 mm × 0.5 mm; **5**, 0.7 mm × 0.2 mm × 0.1 mm) were mounted under an atmosphere of argon in glass capillaries, which were then sealed off. The intensity data were collected at room temperature (**3**) and 213 K (**4** and **5**) in the 2θ range of 3–50° for **3** and 4–52° for

**Table 1.** Crystallographic Data for **3–5**

|  | <b>3</b>  | <b>4</b>  | <b>5</b>  |
|--|---|---|---|
| empirical formula                            | C <sub>22</sub> H <sub>37</sub> O <sub>2</sub> Si <sub>3</sub> Ni <sub>2</sub> In | C <sub>30</sub> H <sub>64</sub> In <sub>2</sub> Ni <sub>2</sub> Si <sub>6</sub> | C <sub>30</sub> H <sub>64</sub> Ga <sub>2</sub> Ni <sub>2</sub> Si <sub>6</sub> |
| fw   | 649.99  | 940.41  | 850.21  |
| space group                                  | P1̄ (No. 2) <sup>16</sup>   | P2 <sub>1</sub> (No. 4) <sup>16</sup>   | P2 <sub>1</sub> /c (No. 14) <sup>16</sup>                                       |
| <i>a</i> (pm)                                | 939.3(1)  | 938.0(1)  | 1391.4(3)   |
| <i>b</i> (pm)                                | 1585.6(2)   | 1667.8(2)   | 1707.3(3)   |
| <i>c</i> (pm)                                | 1926.8(3)   | 1368.9(2)   | 1849.0(4)   |
| α (deg)                                      | 84.60(2)  | 90.00   | 90.00   |
| β (deg)                                      | 89.36(3)  | 95.61(2)  | 106.89(3)   |
| γ (deg)                                      | 89.31(3)  | 90.00   | 90.00   |
| <i>V</i> (10 <sup>-30</sup> m <sup>3</sup> ) | 2856.6(6)   | 2131.2(5)   | 4202(2)   |
| <i>Z</i>                                     | 4   | 2   | 4   |
| temp (K)                                     | 293   | 213   | 213   |
| λ (Å)  | 0.710 73  | 0.710 73  | 0.710 73  |
| ρ <sub>calc</sub> (g cm <sup>-3</sup> )      | 1.511   | 1.465   | 1.344   |
| μ (mm <sup>-1</sup> )                        | 2.246   | 2.125   | 2.340   |
| R1 <sup>a</sup>                              | 0.0403  | 0.0457  | 0.0263  |
| wR2 <sup>b</sup>                             | 0.0769  | 0.0977  | 0.0883  |

<sup>a</sup> R1 = Σ||F<sub>o</sub>| – |F<sub>c</sub>||/Σ|F<sub>o</sub>| (*F* > 4σ(*F*)). <sup>b</sup> wR2 = {Σw(*F*<sub>o</sub><sup>2</sup> – *F*<sub>c</sub><sup>2</sup>)/Σw(*F*<sub>o</sub><sup>2</sup>)<sup>1/2</sup>} (all data).

**4** and **5**, spanning the octants –11 ≤ *h* ≤ 11, –18 ≤ *k* ≤ 18, 0 ≤ *l* ≤ 22; –11 ≤ *h* ≤ 11, –19 ≤ *k* ≤ 20, –16 ≤ *l* ≤ 16; and –17 ≤ *h* ≤ 17, –20 ≤ *k* ≤ 20, –20 ≤ *l* ≤ 20, respectively. A total of 10 040 independent reflections were collected for compound **3** (7594 for **4** and 7707 for **5**). All structures were solved by direct methods using the program system SHELXTL PLUS<sup>15</sup> and refined with the SHELXL-93<sup>15</sup> program via full-matrix least-squares calculations based on *F*<sup>2</sup>. All non-hydrogen atoms were refined with anisotropic displacement parameters; hydrogen atoms were calculated on ideal positions and allowed to ride on the bonded atom with *U* = 1.2*U*<sub>eq</sub>(C). The crystallographic data and details of the final *R* values are provided in Table 1. Conventional *R* factors (R1) are based on *F* using reflections with *F* > 4σ(*F*) (8697 reflections for **3**, 6875 for **4**, and 6201 for **5**); weighted *R* factors (wR2) are based on *F*<sup>2</sup>. The number of refined parameters was 586 (**3**), 378 (**4**), and 437 (**5**). Compound **3** crystallized with two independent molecules in the asymmetric unit. One C(SiMe<sub>3</sub>)<sub>3</sub> group (C1) showed a disorder. The trimethylsilyl groups were refined with occupancy factors of 0.76 and 0.24. A similar disorder was observed for one of the C(SiMe<sub>3</sub>)<sub>3</sub> substituents of compound **5** (C1; occupancy factors 0.86 and 0.14).

**Computational Section.** Geometry optimizations of the model complexes [CpNi{μ–InCH<sub>3</sub>}<sub>2</sub>NiCp] (**4M**) and [CpNi{μ–GaCH<sub>3</sub>}<sub>2</sub>NiCp] (**5M**) representing compounds **4** and **5**, respectively, are performed without symmetry constraints (i.e., in C<sub>1</sub> symmetry) using the combination of density functionals proposed by Becke<sup>17</sup> and Perdew<sup>18</sup> (BP86). A nonrelativistic small-core effective core potential (ECP) and the (441/2111/41) split-valence basis set of Hay and Wadt<sup>19</sup> are used for Ni in conjunction with an all-electron 6-31G(d) basis set for first- and second-row elements.<sup>20</sup> For the heavier group-13 elements Ga and In, we use large-core quasi-relativistic ECPs together with (31/31/1) valence basis sets.<sup>21</sup> These structures are verified to represent local minima on their respective potential energy surface by calculating their harmonic vibrational frequencies at the same level of theory. All calculations

(15) SHELXTL PLUS, release 4.1; Siemens Analytical X-RAY Instruments Inc., Madison, WI, 1990. Sheldrick, G. M. SHELXL-93, Program for the Refinement of Structures; Universität Göttingen: Göttingen, Germany, 1993.

(16) Hahn, T., Ed. *International Tables for Crystallography, Space Group Symmetry*; Kluwer Academic Publishers: Dordrecht, The Netherlands, 1989; Vol. A.

(17) Becke, A. D. *Phys. Rev. A* **1988**, *38*, 3098.

(18) Perdew, J. P. *J. Phys. Rev. B* **1986**, *33*, 8822.

(19) Hay, P. J.; Wadt, W. R. *J. Chem. Phys.* **1985**, *82*, 299.

(20) (a) Hehre, W. J.; Ditchfield, R.; Pople, J. A. *J. Chem. Phys.* **1972**, *56*, 2257. (b) Hariharan, P. C.; Pople, J. A. *Theor. Chim. Acta* **1973**, *28*, 213. (c) Gordon, M. S. *Chem. Phys. Lett.* **1980**, *76*, 163.

(21) Bergner, A.; Dolg, M.; Küchle, W.; Stoll, H.; Preuss, H. *Mol. Phys.* **1993**, *80*, 1431.

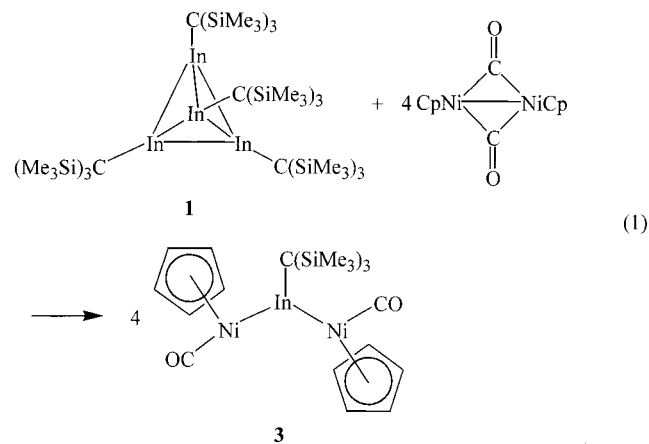
have been carried out with the program package Gaussian98.<sup>22</sup> Cartesian coordinates and structural parameters of all structures optimized are summarized in the Supporting Information.

To assign and describe the bonding situation between the various atoms, particularly between In–In and Ga–Ga, we use the topological analysis of the electronic structure according to Bader's atoms in molecules (AIM) theory<sup>23</sup> and Weinhold's NBO analysis.<sup>24</sup> The numerical data from these analyses are summarized in the Supporting Information (Tables S1 and S2). The basis sets used for these calculations are slightly modified in that small-core quasi-relativistic ECPs and uncontracted 12s11p7d Gaussian-type valence basis sets are used for Ga and In.<sup>22</sup>

## Results and Discussion

**(Me<sub>3</sub>Si)<sub>3</sub>C–In(NiCpCO)<sub>2</sub> (3).** The reactions of octacarbonyldicobalt with tetraindane(4), **1**, afforded two products<sup>10</sup> in which one or both bridging carbonyl ligands were replaced by monomeric InR fragments and which both were isostructural to the starting carbonyl complex. The course of these reactions was determined by the stoichiometric ratio in which the starting compounds were employed. We hoped to realize similar substitution reactions when we treated the dinickel complex Ni<sub>2</sub>Cp<sub>2</sub>(μ-CO)<sub>2</sub> with **1** in different molar ratios. In all cases, an excess of **1** has to be employed for the complete consumption of the nickel compound because **1** partially decomposes by the formation of elemental indium. Furthermore, all products are highly hygroscopic, and the products of hydrolysis could not be separated by repeated recrystallization. In addition to the usual procedure, the predried solvents were therefore further dried over *n*-butyllithium and freshly distilled prior to use.

To replace only one bridging CO ligand, Ni<sub>2</sub>Cp<sub>2</sub>(μ-CO)<sub>2</sub> was treated with **1** in a molar ratio of 1 to 3 in boiling *n*-hexane (eq 1). However, a red solid (**3**) was isolated after recrystallization



that clearly was not the product of a substitution reaction. Its IR spectrum showed two absorptions at 1964 and 1948 cm<sup>-1</sup>, which are in the characteristic range of terminal CO groups. A resonance at δ = 191 ppm in the <sup>13</sup>C NMR spectrum further

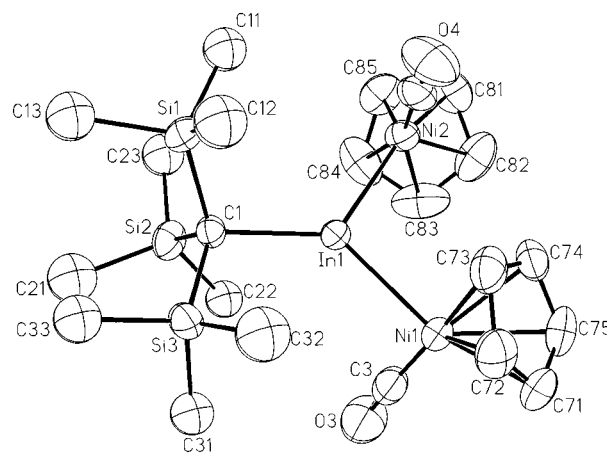


**Figure 1.** Molecular structure and numbering scheme of **3**. The thermal ellipsoids are drawn at the 40% probability level, hydrogen atoms are omitted for clarity, and the carbon atom C4 of the carbonyl group attached to Ni2 is not named.

**Table 2.** Important Bond Lengths (pm) and Angles (deg) for **3**

| molecule 1        |            | molecule 2        |            |
|-------------------|------------|-------------------|------------|
| In(1)–C(1)        | 223.3(4)   | In(2)–C(2)        | 224.8(4)   |
| In(1)–Ni(1)       | 251.23(9)  | In(2)–Ni(3)       | 251.78(9)  |
| In(1)–Ni(2)       | 251.88(10) | In(2)–Ni(4)       | 252.01(10) |
| Ni(1)–C(3)        | 170.4(6)   | Ni(3)–C(5)        | 168.8(6)   |
| Ni(2)–C(4)        | 168.9(6)   | Ni(4)–C(6)        | 169.0(6)   |
| C(3)–O(3)         | 114.9(6)   | C(5)–O(5)         | 116.2(6)   |
| C(4)–O(4)         | 116.3(6)   | C(6)–O(6)         | 115.1(6)   |
| C(1)–In(1)–Ni(1)  | 131.6(1)   | C(2)–In(2)–Ni(3)  | 129.3(1)   |
| C(1)–In(1)–Ni(2)  | 125.0(1)   | C(2)–In(2)–Ni(4)  | 127.6(1)   |
| Ni(1)–In(1)–Ni(2) | 103.36(3)  | Ni(3)–In(2)–Ni(4) | 103.05(3)  |
| In(1)–Ni(1)–C(3)  | 89.6(2)    | In(2)–Ni(3)–C(5)  | 88.8(2)    |
| In(1)–Ni(2)–C(4)  | 83.8(2)    | In(2)–Ni(4)–C(6)  | 84.5(2)    |

verified the existence of terminal CO ligands. The integration ratio of the <sup>1</sup>H NMR spectrum showed that the product contained one C(SiMe<sub>3</sub>)<sub>3</sub> substituent per two cyclopentadienyl ligands.

The molecular structure of **3** is depicted in Figure 1. It has a central In atom coordinated by an alkyl group and two NiCp(CO) moieties each with a terminal CO ligand. Thus, an unprecedented reaction of **1** occurred in which one InR group was inserted into the Ni–Ni bond of the starting nickel complex. While such a behavior is quite unusual for the alkylgallium(I) and alkylindium(I) derivatives, which in many cases gave substitution reactions as described above, the insertion of indium(I) halides into metal–metal bonds of transition metal compounds has been observed several times before.<sup>25</sup> Thus, for the first time InR did not behave as a carbonyl analogous compound here. The In atom of **3** has a planar coordination sphere (sum of the angles is 360.0°; see Table 2). The Ni–In distances (251.7 pm on average) are in the expected range for unsupported Ni–In bonds.<sup>26</sup> Larger separations were observed for bridged bonds,<sup>27</sup> while a considerably shorter bond length (231.0 pm) was observed in the tetracarbonylnickel analogous

(22) Frisch, M. J.; Trucks, G. W.; Schlegel, H. B.; Scuseria, G. E.; Robb, M. A.; Cheeseman, J. R.; Zakrzewski, V. G.; Montgomery, J. A., Jr.; Stratmann, R. E.; Burant, J. C.; Dapprich, S.; Millam, J. M.; Daniels, A. D.; Kudin, K. N.; Strain, M. C.; Farkas, O.; Tomasi, J.; Barone, V.; Cossi, M.; Cammi, R.; Mennucci, B.; Pomelli, C.; Adamo, C.; Clifford, S.; Ochterski, J.; Petersson, G. A.; Ayala, P. Y.; Cui, Q.; Morokuma, K.; Malick, D. K.; Rabuck, A. D.; Raghavachari, K.; Foresman, J. B.; Cioslowski, J.; Ortiz, J. V.; Stefanov, B. B.; Liu, G.; Liashenko, A.; Piskorz, P.; Komaromi, I.; Gomperts, R.; Martin, R. L.; Fox, D. J.; Keith, T.; Al-Laham, M. A.; Peng, C. Y.; Nanayakkara, A.; Gonzalez, C.; Challacombe, M.; Gill, P. M. W.; Johnson, B. G.; Chen, W.; Wong, M. W.; Andres, J. L.; Head-Gordon, M.; Replogle, E. S.; Pople, J. A. *Gaussian 98*, revision A.3; Gaussian, Inc.: Pittsburgh, PA, 1998.

(23) (a) Bader, R. F. W. *Atoms in Molecules: A Quantum Theory*; Oxford University Press: Oxford, 1990. (b) Bader, R. F. W. *Chem. Rev.* **1991**, *91*, 893. (c) The set of programs used is available at <http://www.chemistry.mcmaster.ca/aimpac/>.

(24) Reed, A. E.; Curtiss, L. A.; Weinhold, F. *Chem. Rev.* **1988**, *88*, 899.

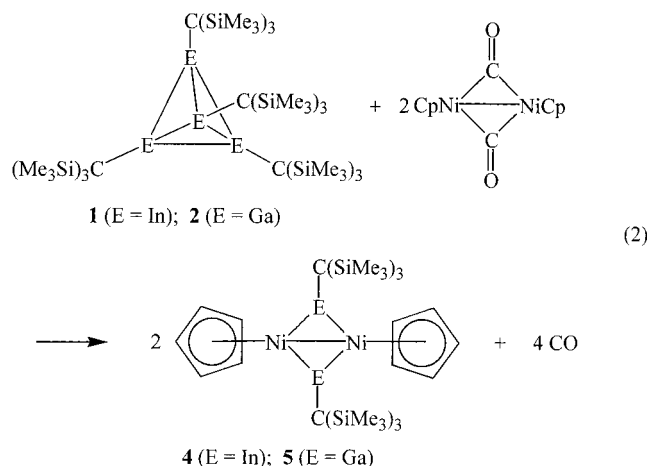
(25) (a) Clarkson, L. M.; Norman, N. C.; Farrugia, L. J. *J. Organomet. Chem.* **1990**, *390*, C10. (b) Hsieh, A. T. T.; Mays, M. J. *Inorg. Nucl. Chem. Lett.* **1971**, *7*, 223.

(26) (a) Fischer, R. A.; Herdtweck, E.; Priermeier, T. *Inorg. Chem.* **1994**, *33*, 934. (b) Weiss, J.; Priermeier, T.; Fischer, R. A. *Inorg. Chem.* **1996**, *35*, 71. (c) Weiss, J.; Frank, A.; Herdtweck, E.; Nlate, S.; Mattner, M.; Fischer, R. A. *Chem. Ber.* **1996**, *129*, 297.

derivative Ni[InC(SiMe<sub>3</sub>)<sub>3</sub>]<sub>4</sub>,<sup>12,13</sup> for which an important contribution of π back-bonding was verified by quantumchemical calculations.<sup>12</sup> Thus, the Ni–In bonds of **3** seem to be less influenced by a π contribution, probably owing to the competition between InR and the good π acceptor ligands cyclopentadienyl and carbonyl. The In–C bond lengths (224.1 pm on average) are similar to those found in **1**,<sup>1</sup> but they are longer than those usually observed in transition metal compounds bearing the InR ligand (<220 pm).<sup>7–10</sup> The shortening of the E–C bonds (E = Al, Ga, In) in such complexes was interpreted in terms of a more ionic interaction between the indium and transition metal atoms and an enhancement of the positive charge at the third main-group elements.<sup>28</sup> The longer bonds in **3** may be caused by a lower charge separation or a strong steric repulsion between the bulky alkyl substituents and the NiCp(CO) groups.

The Ni–C distances to the CO ligands are very short (169.3 pm on average) compared to those of the bridging groups in the starting carbonyl complex (190 pm)<sup>29</sup> or to those of Ni(CO)<sub>4</sub> (184 pm).<sup>30</sup> This observation may reflect the strong π back-donation of electron density from each nickel atom to the single CO ligand and was reported before for several other complexes with a comparable bonding situation.<sup>26,29,31,32</sup> In contrast, the distances between the Ni atoms and the centers of the cyclopentadienyl rings (174.9 pm) are quite normal; in most cases they are only slightly influenced by the different coordination spheres.<sup>26,29,31,32</sup>

[CpNi{μ-InC(SiMe<sub>3</sub>)<sub>3</sub>]<sub>2</sub>NiCp] (**4**) and [CpNi{μ-GaC(SiMe<sub>3</sub>)<sub>3</sub>]<sub>2</sub>NiCp] (**5**). In further reactions, we enhanced the concentration of tetraindane(4) **1** (eq 2). Once again, part of



the indium compound decomposed by the precipitation of a metallic gray powder, and we needed an excess of **1** to consume the starting compounds and intermediates completely (see

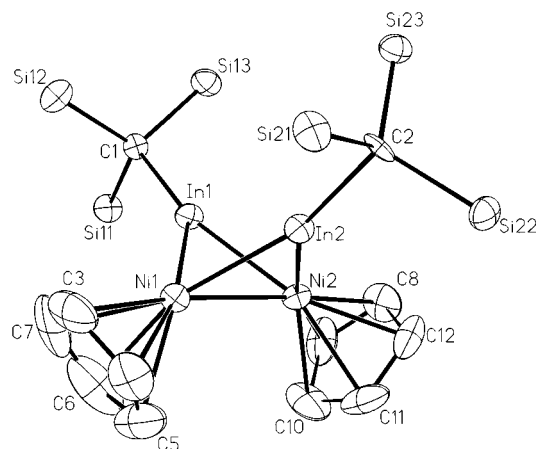


**Figure 2.** Molecular structure and numbering scheme of **4**. The thermal ellipsoids are drawn at the 40% probability level, and methyl groups and hydrogen atoms are omitted for clarity.

**Table 3.** Important Bond Lengths (pm) and Angles (deg) for **4<sup>a</sup>**

|                   |          |              |                   |           |              |
|-------------------|----------|--------------|-------------------|-----------|--------------|
| In(1)–C(1)        | 218.9(8) | <i>216.3</i> | In(2)–C(2)        | 221.6(7)  | <i>216.3</i> |
| In(1)–Ni(1)       | 244.5(1) | <i>244.5</i> | In(2)–Ni(1)       | 243.8(1)  | <i>244.8</i> |
| In(1)–Ni(2)       | 244.1(1) | <i>244.8</i> | In(2)–Ni(2)       | 244.7(1)  | <i>244.5</i> |
| Ni(1)–Ni(2)       | 249.1(1) | <i>258.9</i> | In(1)–In(2)       | 332.49(9) | <i>338.5</i> |
| In(1)–Ni(1)–In(2) | 85.84(4) | <i>87.5</i>  | In(1)–Ni(2)–In(2) | 85.71(4)  | <i>87.5</i>  |
| Ni(1)–In(1)–Ni(2) | 61.32(4) | <i>63.9</i>  | Ni(1)–In(2)–Ni(2) | 61.32(4)  | <i>63.9</i>  |
| C(1)–In(1)–Ni(1)  | 146.5(2) | <i>148.7</i> | C(2)–In(2)–Ni(1)  | 153.5(2)  | <i>147.4</i> |
| C(1)–In(1)–Ni(2)  | 151.6(2) | <i>147.4</i> | C(2)–In(2)–Ni(2)  | 145.2(2)  | <i>148.7</i> |

<sup>a</sup> Calculated values for the model complex **4M** are given in italics.

below). A product (**4**) was formed that, owing to its <sup>1</sup>H NMR spectrum, had one cyclopentadienyl group per C(SiMe<sub>3</sub>)<sub>3</sub> substituent and for which equivalent molar amounts of nickel and indium were determined by elemental analysis. No absorptions of CO ligands were detected in the IR spectrum, so surprisingly all carbonyl groups seemed to be removed.

The crystal structure determination of **4** revealed a structure that is isostructural to the starting carbonyl complex with two InR ligands bridging a couple of Ni atoms in a butterfly conformation (Figure 2). A similar compound with bridging Al atoms Ni<sub>2</sub>Cp<sub>2</sub>(μ-AlCp\*)<sub>2</sub> was obtained before by the reaction of nickelocene with the aluminum(I) compound Al<sub>4</sub>Cp\*<sub>4</sub>.<sup>33</sup> The Ni–Ni distance (249.1 pm, Table 3) is lengthened compared to that of the starting compound Ni<sub>2</sub>Cp<sub>2</sub>(μ-CO)<sub>2</sub> (235.5 pm).<sup>29</sup> A similar lengthening of metal–metal distances compared to distances in pure carbonyl complexes was observed in all transition metal compounds with bridging InR groups.<sup>7–10</sup> It may be caused by the larger covalence radius of indium atoms compared to that of carbon atoms, which by longer bond lengths to the bridging atoms allow a larger metal–metal separation. The Ni–In distances (244.3 pm on average) are in the lower range of values known from literature<sup>26,27</sup> but are not as short as in the Ni(CO)<sub>4</sub> analogous compound Ni[InC(SiMe<sub>3</sub>)<sub>3</sub>]<sub>4</sub>.<sup>12,13</sup> The shortening compared to compound **3** may be caused by the particular bonding situation of the butterfly structure of **4** with the requirement of the pairing of the nickel electrons by a direct Ni–Ni bond or by multicenter interactions (see quantum chemical calculations below). A rather small In–In separation (332.5 pm) results, which is longer than that observed for tetraindane(4), **1** (300.2 pm), but smaller than in some indium(I) cyclopentadienide derivatives (>360 pm) with pseudodimeric<sup>34</sup> or hexameric structures<sup>35</sup> and weak dispersive In–In

- (27) (a) Demartin, F.; Iapalucci, M. C.; Longoni, G. *Inorg. Chem.* **1993**, *32*, 5536. (b) Marsh, R. E.; Bernal, I. *Acta Crystallogr., Sect. B* **1995**, *51*, 300.
- (28) (a) Üffing, C.; Ecker, A.; Köppe, R.; Schnöckel, H. *Organometallics* **1998**, *17*, 2373. (b) Yu, Q.; Purath, A.; Donchev, A.; Schnöckel, H. *J. Organomet. Chem.* **1999**, *584*, 94. (c) Boehme, C.; Frenking, G. *Chem.–Eur. J.* **1999**, *5*, 2184.
- (29) Madach, T.; Fischer, K.; Vahrenkamp, H. *Chem. Ber.* **1980**, *113*, 3235.
- (30) (a) Hedberg, L.; Iijima, T.; Hedberg, K. *J. Chem. Phys.* **1979**, *70*, 3224. (b) Ladell, J.; Post, B.; Fankuchen, I. *Acta Crystallogr.* **1952**, *5*, 795.
- (31) (a) Carre, F. H.; Corriu, R. J. P.; Henner, B. J. L. *J. Organomet. Chem.* **1982**, *228*, 139. (b) Akita, M.; Kondoh, A.; Moro-oka, Y. *J. Chem. Soc., Dalton Trans.* **1989**, 1627.
- (32) (a) Fischer, R. A.; Behm, J.; Herdtweck, E.; Kronseder, C. *J. Organomet. Chem.* **1992**, *437*, C29. (b) Hoffmann, H.; Fischer, R. A.; Antelmann, B.; Huttner, G. *J. Organomet. Chem.* **1999**, *584*, 131.

- (33) Dohmeier, C.; Krautscheid, H.; Schnöckel, H. *Angew. Chem.* **1994**, *106*, 2570; *Angew. Chem., Int. Ed. Engl.* **1994**, *33*, 2482.

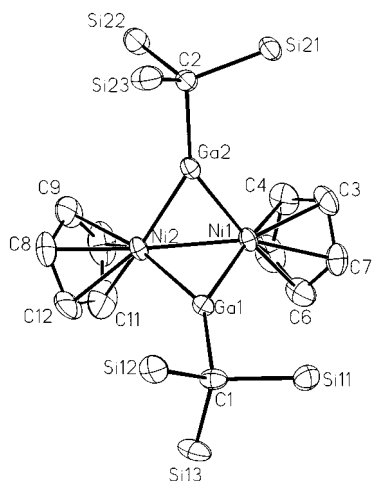


**Figure 3.** Molecular structure and numbering scheme of **5**. The thermal ellipsoids are drawn at the 40% probability level, and methyl groups and hydrogen atoms are omitted for clarity.

interactions.<sup>36</sup> A similar short distance (336.2 pm) was observed in the compound  $\text{Co}_2(\text{CO})_6[\mu\text{-InC}(\text{SiMe}_3)_3]_2$ ,<sup>10</sup> while in most such cases long distances of 360–380 pm were determined.<sup>8,9</sup> The separation between the nickel atoms and the center of the cyclopentadienyl ligands is 173.2 pm. The angle between the  $\text{Ni}_2\text{In}$  triangles is  $104^\circ$ , which is smaller than that of the carbonyl derivative ( $142^\circ$ ).<sup>29</sup> The indium atoms have an almost ideally planar coordination sphere (sum of the angles is  $359.4^\circ$ ).

Thus, we observed a rather strange reaction between  $\text{Ni}_2\text{Cp}_2(\mu\text{-CO})_2$  and tetraindane(**4**), **1**. In the first step, InR did not replace a bridging carbonyl ligand as often observed before but was inserted into the Ni–Ni bond. Both CO groups of the product **3** occupied terminal positions, and the Ni atoms were separated by a large distance of almost 400 pm. The addition of a further equivalent of InR led to the complete loss of all carbonyl groups. A product (**4**) was formed in which the Ni atoms approach a distance similar to that of the starting carbonyl complex and which is isostructural to the carbonyl compound with two InR ligands in a bridging position between both Ni atoms. The occurrence of compound **3** as an intermediate in the course of the formation of **4** was verified by  $^1\text{H}$  NMR spectroscopy, and it seems that terminally coordinated CO groups were replaced by InR ligands, which was observed before only for the reaction of **1** with  $\text{Mn}_2(\text{CO})_{10}$ .<sup>7</sup> These observations verify the well-balanced and remarkable bonding situation in such transition metal complexes bearing CO and ER ligands ( $E = \text{Ga}, \text{In}$ ), which is discussed in more detail below.

The reaction of the tetragallium compound **2** with  $\text{Ni}_2\text{Cp}_2(\mu\text{-CO})_2$  is different from that of the indium analogue **1** (eq 2). Independent of the stoichiometric ratio of the starting compounds, the product of the insertion of GaR into the Ni–Ni bond has never been observed. Instead, the product of the complete substitution of both CO ligands (**5**) analogous to **4** was formed as the only detectable compound in all cases, and the excess of the carbonyl nickel complex could be recovered. The spectroscopic findings are quite similar to those of the indium analogue **4** and need no further discussion. The molecular structure of **5** is depicted in Figure 3. **4** and **5** are not

**Table 4.** Important Bond Lengths (pm) and Angles (deg) for **5**<sup>a</sup>

|                   |           |       |                   |           |       |
|-------------------|-----------|-------|-------------------|-----------|-------|
| Ga(1)–C(1)        | 199.2(2)  | 202.2 | Ga(2)–C(2)        | 199.7(3)  | 202.2 |
| Ga(1)–Ni(1)       | 227.56(6) | 230.1 | Ga(2)–Ni(1)       | 227.89(6) | 230.1 |
| Ga(1)–Ni(2)       | 227.69(6) | 230.1 | Ga(2)–Ni(2)       | 227.56(9) | 230.1 |
| Ni(1)–Ni(2)       | 244.85(7) | 255.0 | Ga(1)–Ga(2)       | 302.88(9) | 310.0 |
| Ga(1)–Ni(1)–Ga(2) | 83.36(2)  | 84.7  | Ga(1)–Ni(2)–Ga(2) | 83.41(2)  | 84.7  |
| Ni(1)–Ga(1)–Ni(2) | 65.07(2)  | 67.3  | Ni(1)–Ga(2)–Ni(2) | 65.04(2)  | 67.3  |
| C(1)–Ga(1)–Ni(1)  | 147.68(9) | 146.6 | C(2)–Ga(2)–Ni(1)  | 146.89(8) | 146.6 |
| C(1)–Ga(1)–Ni(2)  | 146.85(9) | 146.0 | C(2)–Ga(2)–Ni(2)  | 147.34(8) | 146.0 |

<sup>a</sup> Calculated values for the model complex **5M** are given in italics.

isotypic, but their structures with both Ni atoms bridged by E–R groups in a butterfly arrangement differ only slightly. The Ni–Ni distance (244.85 pm, Table 4) is slightly shorter than that of **4** in accordance with the smaller covalence radius of gallium compared to indium. The Ni–Ga distances (227.7 pm on average) are similar to those observed before,<sup>32,37</sup> but only very few organoelement compounds containing Ni–Ga bonds were published up to now. As expected, they are longer than those of the  $\text{Ni}(\text{CO})_4$  analogous compounds  $\text{Ni}[\text{GaC}(\text{SiMe}_3)_3]_4$  (217.0 pm)<sup>12</sup> and  $\text{Ni}(\text{GaCp}^*)_4$  (221.9 pm).<sup>38</sup> The Ga–Ga separation is short (302.9 pm; 268.8 pm in **2**), but a bonding interaction between the Ga atoms has to be excluded (see below). The normals of the  $\text{Ni}_2\text{Ga}$  planes enclose an angle of  $104^\circ$ . The Ga–C distances (199.5 pm) are considerably smaller than those of **2** (208 pm).<sup>3</sup>

### Computational Results

**[CpNi{ $\mu\text{-InCH}_3$ } $_2$ NiCp] (4M) and [CpNi{ $\mu\text{-GaCH}_3$ } $_2$ NiCp] (5M).** The calculated structural parameters of the model complexes **4M** and **5M** are in reasonable good agreement with their experimental analogues found for complexes **4** and **5**. The more significant deviations only occur for the calculated Ni–Ni bond lengths, which are predicted to be 10 pm longer than the experimental values. The agreement between theory and experiment becomes better for the calculated Ni–In and Ni–Ga bond lengths of **4M** and **5M**. The differences decrease to 7 and 6 pm, respectively, and drop to less than 3 pm for the calculated In–C and Ga–C bond lengths. In a second set of geometry optimizations we find that a relativistic approach like the zeroth-order regular approximation (ZORA)<sup>39</sup> implemented in the ADF99 suite of programs<sup>40</sup> sporadically yields refined structural parameters. While these calculations give Ga–Ni, Ga–Ga, and Ga–C bond lengths of **5M**, which differ from the experimental values by less than 1 pm, the deviations of the already overestimated Ni–Ni bond length are, however, in-

(34) Schumann, H.; Janiak, C.; Görlitz, F.; Loebel, J.; Dietrich, A. *J. Organomet. Chem.* **1989**, *363*, 243.

(35) Beachley, O. T., Jr.; Churchill, M. R.; Fettingner, J. C.; Pazik, J. C.; Victoriano, L. *J. Am. Chem. Soc.* **1986**, *108*, 4666.

(36) (a) Janiak, C.; Hoffmann, R. *J. Am. Chem. Soc.* **1990**, *112*, 5924. (b) Schwerdtfeger, P. *Inorg. Chem.* **1991**, *30*, 1660.

(37) Jutzi, P.; Neumann, B.; Reumann, G.; Stammler, H.-G. *Organometallics* **1998**, *17*, 1305.

(38) Jutzi, P.; Neumann, B.; Schebaum, L. O.; Stammler, A.; Stammler, H.-G. *Organometallics* **1999**, *18*, 4462.

(39) (a) van Lenthe, E.; Baerends, E. J.; Snijders, J. G. *J. Chem. Phys.* **1993**, *99*, 4597. (b) van Lenthe, E.; Baerends, E. J.; Snijders, J. G. *J. Chem. Phys.* **1994**, *101*, 9783. (c) van Lenthe, E.; Snijders, J. G.; Baerends, E. J. *J. Chem. Phys.* **1996**, *105*, 6505. (d) van Lenthe, E.; van Leeuwen, R.; Baerends, E. J.; Snijders, J. G. *Int. J. Quantum Chem.* **1996**, *57*, 281. (e) van Lenthe, E.; Ehlers, A. E.; Baerends, E. J. *J. Chem. Phys.* **1999**, *110*, 8943.

(40) (a) Baerends, E. J.; Bérces, A.; Bo, C.; Boerrigter, P. M.; Cavallo, L.; Deng, L.; Dickson, R. M.; Ellis, D. E.; Fan, L.; Fischer, T. H.; Fonseca Guerra, C.; van Gisbergen, S. J. A.; Groeneveld, J. A.; Gritsenko, O. V.; Harris, F. E.; van den Hoek, P.; Jacobsen, H.; van Kessel, G.; Kootstra, F.; van Lenthe, E.; Osinga, V. P.; Philipsen, P. H. T.; Post, D.; Pye, C. C.; Ravenek, W.; Ros, P.; Schipper, P. R. T.; Schreckenbach, G.; Snijders, J. G.; Sola, M.; Swerhone, D.; te Velde, G.; Vernooijs, P.; Versluis, L.; Visser, O.; van Wezenbeek, E.; Wiesenker, G.; Wolff, S. K.; Woo, T. K.; Ziegler, T. ADF, 1999. (b) Fonseca Guerra, C.; Snijders, J. G.; te Velde, G.; Baerends, E. *J. Theor. Chem. Acc.* **1998**, *99*, 391.

creased. In addition, structural parameters obtained for **4M** deviate from the calculated data given in the text in that they are generally longer by 2–3 pm. Details of these calculations and Cartesian coordinates of the optimized geometries are given in the Supporting Information. We note that the calculated structures, although optimized without symmetry constraints, are very close to  $C_2$  and  $C_{2v}$  symmetry. Note, however, that the use of such symmetry constraints in the geometry optimization process does not result in structures that represent local minima on the respective potential energy surfaces.

The numerical results obtained from the Bader analysis are summarized in the Supporting Information (Table S1) and are visualized by the contour-line diagram shown in Figure 4. The data reveal a consistent picture of the bonding situation within the tetrahedral arrangement involving Ni and the respective group-13 metals of the two model complexes **4M** and **5M**. That is, we do not find evidence for a bonding interaction between In–In or Ga–Ga! No suitable bond critical point between group-13 elements could be located. Therefore, we suggest a butterfly structure similar to the structure of the starting carbonyl compound as the appropriate binding model for the structural description of these complexes. Furthermore, the moderate to low numerical values of the electron density  $\rho(\mathbf{r}_b)$  obtained for the Ni–Ni, Ni–In, and Ni–Ga bonds in conjunction with highly positive values for the corresponding Laplacians  $\nabla^2\rho(\mathbf{r}_b)$  indicate a predominant closed-shell interaction between the metals.<sup>23a</sup> This is also in line with the relatively small negative values of the energy densities  $H(\mathbf{r}_b)$ , which are close to zero, thus ruling out *significant* covalent character in these bonds. In comparison to that, the high (and negative) values of the energy densities found for In–C and Ga–C bonds suggest covalent contributions of these bonds, which is in line with a charge concentration around the carbon atoms as it is shown in the contour-line diagram (Figure 4).

The partial charges derived from the NBO analysis are summarized in the Supporting Information (Table S2). These values indicate positive charges on all metal atoms, whereas the partial charges of C and H sum to negatively charged ligands  $\text{C}_5\text{H}_5$  and  $\text{CH}_3$ . The overall effect of this distribution is negatively charged Ni– $\text{C}_5\text{H}_5$  and equally positively charged Ga– $\text{CH}_3$  and In– $\text{CH}_3$  complex fragments. The positive charge on the group-13 elements is always larger than on Ni. These moderate to high positive charges are supported by the AIM data, which indicate charge depletion ( $\nabla^2\rho(\mathbf{r}_b) > 0$ , dashed lines in Figure 4) between these metals. A detailed examination of the orbital contributions and thus of the donor–acceptor characteristics, particularly the  $p(\pi)$  acceptor capabilities of the Ga– $\text{CH}_3$  and In– $\text{CH}_3$  fragments, is prevented because of the structure of the complexes. Because of the  $C_1$  symmetry, there is no mirror plane, and thus, it is not possible to unequivocally assign a distinct and pure  $p(\pi)$  acceptor orbital for Ga or In.

**Acknowledgment.** We are grateful to the Deutsche Forschungsgemeinschaft and the Fonds der Chemischen Industrie for generous financial support. We acknowledge excellent service by the Hochschulrechenzentrum of the Philipps-Universität Marburg and the HHLR Darmstadt.

**Supporting Information Available:** Cartesian coordinates of the optimized geometries, electron density data, and partial charges from the NBO analysis of the model complexes **4M** and **5M** and X-ray crystallographic files in CIF format for complexes  $(\text{Me}_3\text{Si})_3\text{C}-\text{In}[\text{NiCp}-$

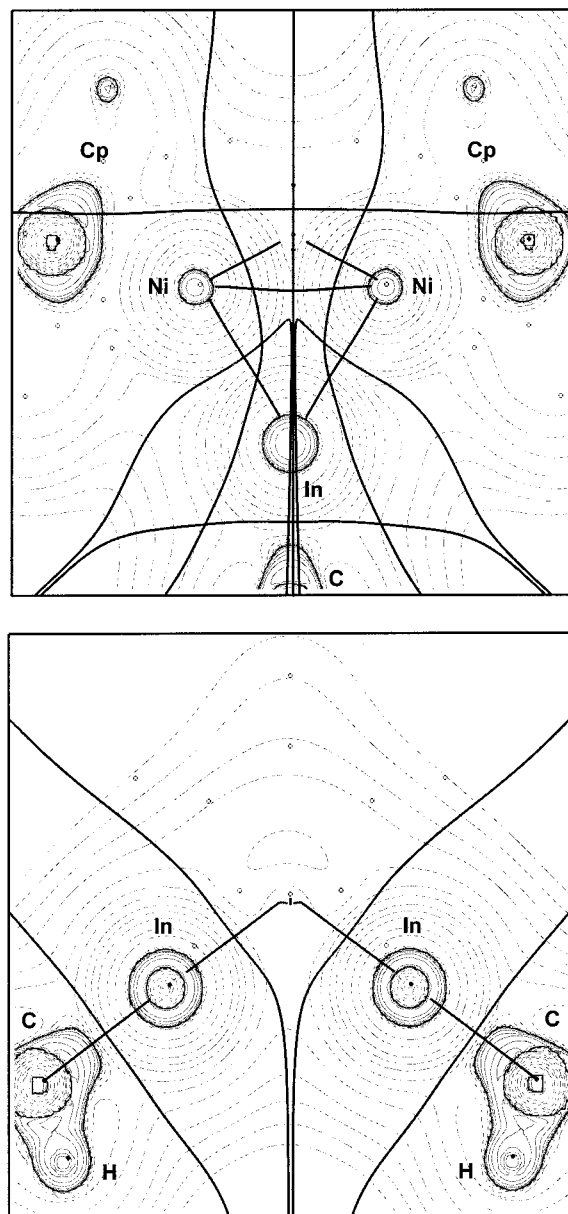


**Figure 4.** Contour-line diagram of the Laplacian distribution  $\nabla^2\rho(\mathbf{r}_{\text{BCP}})$ . Dashed lines ( $\nabla^2\rho(\mathbf{r}_{\text{BCP}}) > 0$ ) indicate regions of charge depletion, and solid lines ( $\nabla^2\rho(\mathbf{r}_{\text{BCP}}) < 0$ ) indicate regions of charge concentration. Solid lines connecting atom centers represent bond paths, whereas solid lines separating the atom centers indicate the zero-flux surfaces in the molecular plane. Crossing points between bond paths and the zero-flux surface are bond critical points (BCPs). Because of the similarity between the plots obtained of the In- and Ga-model complexes, the figure only shows the contour-line diagram for the former complex viewed from the Ni–Ni–In–C plane (top) and the C–In–In–C plane (bottom).

$(\text{CO})_2$ , **3**,  $[\text{CpNi}\{\mu\text{-InC}(\text{SiMe}_3)_3\}_2\text{NiCp}]$ , **4**, and  $[\text{CpNi}\{\mu\text{-GaC}(\text{SiMe}_3)_3\}_2\text{NiCp}]$ , **5**. This material is available free of charge via the Internet at <http://pubs.acs.org>. Further details of the crystal structure determinations are also available from the Cambridge Crystallographic Data Center on quoting the depository numbers CCDC-144775 (**3**), CCDC-144776 (**4**), and CCDC-144777 (**5**).

IC0005947